Uniaxial compressive behavior of scrapped tire and sand-filled wire netted geocell with a geotextile envelope

Stéphane Lambert, François Nicot, Philippe Gotteland

Uniaxial compressive behavior of scrapped tire and sand-filled wire netted geocell with a geotextile envelope

Stéphane Lambert [a,*], François Nicot [a], Philippe Gotteland [b]

[a] Cemagref, UR ETGR, F-38402 St-Martin d'Hères, France
[b] 3SR, UJF-INPG-CNRS-UMR5521, DU Grenoble Universités, 38041 Grenoble cedex 9, France

Cellular structures are widely used in civil engineering. Their design is based on the understanding of the mechanical behavior of geocells. This paper investigates the response of a single geocell to a uniaxial compression test. The geocells were cubic, either 500 mm or 300 mm on a side. The fill materials were sand and scrapped tire and sand mixtures in different mass ratios. The envelope of the geocell was made up of a hexagonal wire netting cage and a containment geotextile. The response of the geocell is dis-cussed based on the axial load and displacement measurements as well as the change in geocell volume. The axial load was found to be globally governed by the interaction between the fill material and the envelope, which depends on the shape of the wire mesh and the volumetric behavior of the fill material.

1. Introduction

The principle of associating a soil with a man-made envelope to create a reinforced structure was first applied in the 2nd century B.C. for military applications and mainly for rapid repair of fortifications. Based on this principle, gabion cages made of metallic wire netting were developed at the end of the 19th century. In the late 1970s, the US Army Corps of Engineers re-investigated the original principle with the aim of stabilizing beach sand for roadways (Webster, 1979), the first steps towards the development of geocells. Nowadays, geocells are defined as three-dimensional and permeable structures made of alternately linked strips of geotextiles or any planar polymeric products such as HDPE sheets. To a large extent, gabions can be likened to geocells and both are used to build cellular structures.

Cellular structures fulfill various functions in civil engineering applications. For reinforcement purposes, cellular structures are used to build flexible gravity walls, retaining structures, and rockfall protection embankments (Nicot et al., 2007; Chen and Chiu, 2008). Geocells are more specifically used for the reinforcement of base courses over weak subgrades (Yuu et al., 2008). Cellular structures can also serve as building blast protection structures (Scherbatiuk et al., 2008). In hydraulics, cellular structures are used to build weirs (Peyras et al., 1992) to protect banks against erosion and scour and also as components of rapid-deployment flood protection structures (Turk, 2001).

The design of cellular structures must account for the prevailing mechanisms, which are related to the fill material–cell envelope interaction and to the interaction between individual cells (Wesseloo et al., 2009). The interaction between adjoining and interconnected single geocells has been thoroughly investigated with respect to base reinforcement of roads on soft subgrades and embankments (Yuu et al., 2008; Pokharel et al., 2010; Zhang et al., 2010). On the other hand, the number of published studies investigating the interaction between the envelope and the fill material is rather limited. In addition, given the variety of (a) the possible fill material, (b) the envelope's mechanical characteristics, and (c) the geocell's cross-sectional shapes, this interaction is expected to vary greatly from one type of geocell to another.

The interaction between an envelope and a soil was first investigated by Henkel and Gilbert (1952). The aim was to correct triaxial test results depending on the characteristics of the membrane used to contain the tested clayey specimen. These authors proposed a model based on elastic membrane theory to account for the effect of the envelope on the fill material. This effect was considered to be equivalent to an additional confining pressure, $\Delta\sigma_3$, such that:

* Corresponding author. Tel.: +33 4 76 76 27 94; fax: +33 4 76 51 38 03.
E-mail address: stephane.lambert@cemagref.fr (S. Lambert).

$$\Delta\sigma_3 = \frac{2M}{D_0}\left(\frac{1-\sqrt{1-\varepsilon_a}}{1-\varepsilon_a}\right) \quad (1)$$

where D_0 is the initial diameter of the specimen, M is the tensile modulus of the envelope, and ε_a is the axial strain of the specimen.

To establish this model, Henkel and Gilbert (1952) mainly assumed that the specimen remains a right cylinder of constant volume throughout the test.

Eq. (1) was used by different authors who investigated the effect of an envelope on the contained soil for the design of cellular structures.

Many authors also observed that the geocell envelope has no effect on the friction angle, ϕ, of the contained material but modifies the overall cohesion (e.g., Bathurst and Rajagopal, 1993; Iizuka et al., 2004). For a granular and noncohesive material, and assuming that the plastic limit is reached, Bathurst and Rajagopal (1993) proposed for this apparent cohesion, C_a:

$$C_a = \frac{\Delta\sigma_3}{2}\tan\left(\frac{\pi}{4}+\frac{\phi}{2}\right) \quad (2)$$

It is worth highlighting that this equation should not be used for low strains because the plastic limit is reached at larger strains in the presence of the envelope (Bathurst and Rajagopal, 1993; Rajagopal et al., 1999).

The effect of the envelope is similar to an increasing confining pressure, acting therefore on the volume behavior. A thorough analysis of the available experimental results shows that the geocell's carrying capacity starts increasing concomitantly to the decrease in geocell volume (Bathurst and Rajagopal, 1993; Iizuka et al., 2004). Iizuka et al. (2004) noted that the volume effect is more pronounced when the initial soil density is higher. These authors developed a numerical model based on Drucker–Prager's model to account for the influence of the soil dilatancy on the geocell's response.

Moreover, the envelope's confining effect also depends on the initial form of the geocell and on the orientation on the loading. In the case of a cylindrical geocell, the confining effect appears starting with a 10% axial strain if the load is oriented along its diameter (Iizuka et al., 2004), whereas it appears at the beginning of compression if the load is axially oriented (Bathurst and Rajagopal, 1993).

The interaction between the envelope and the fill material thus appears to depend on many parameters. Nevertheless, the complexity of this interaction is often not considered for the design of cellular structures. Indeed, Eq. (1) is generally used for any type of envelope, fill material, or geocell cross-sectional shape (Bathurst and Rajagopal, 1993; Rajagopal et al., 1999; Madhavi Latha et al., 2006).

In view of a proper design of rockfall protection structures using geocells (Nicot et al., 2007; Lambert et al., 2009; Bourrier et al., 2010), a thorough analysis of the interaction between the fill material and the envelope is necessary. The geocells studied are cubic and made up of a hexagonal wire netting mesh envelope filled with different sand and scrapped tire mixtures. While the dynamic response of these cells was studied by the authors in a previous paper (Lambert et al., 2009), this paper addresses their response to static uniaxial compression by investigating the influence of certain characteristics related to both the envelope and the fill material. The results are presented and discussed, with special attention paid to the system's volumetric behavior. The aim is to understand the interaction between the envelope and the fill material, accounting for their specific characteristics. The conditions for an optimum use of such cells in structures exposed to impacts are also discussed.

2. Materials and methods

2.1. Cages, geotextile, and fill material

The cells were made of a metallic wire netting cage, a containment geotextile and the fill material.

The wire netting cages were cubic, with a typical initial height of either 500 mm or 300 mm. These cages can be regarded as a section of the commonly used gabion cages. Indeed, gabions are generally parallelepiped-like cages measuring 1 m × 1 m × 3 m ($W \times H \times L$) whose inner volume is segmented into three cubic sections by square wire netting panels called diaphragms (Fig. 1).

The cages were made from hexagonal wire mesh. A mesh consists of interconnected single wires and double-twisted wires (Fig. 2(a)). It is defined by its width, w, height, h, and by the angle α. Typically, α equals 43° for an undeformed mesh. Table 1 gives the main commercial descriptive characteristics of the different meshes used.

An important feature of this type of wire mesh is that bending at the wire connections results in much larger mesh deformations than those stemming from tensile wire strains (Bergado et al., 2001; Muhunthan et al., 2005). In most practical loading path cases, the amplitude of the mesh deformation mainly results from bending at the wire connections. Assuming that the length of the double and single wires, respectively l_1 and l_2, remain constant (Fig. 2(a)), only parameter α is sufficient to describe the mesh deformation. An increase in α leads to a decrease in h and an increase in w and inversely (Fig. 2(b)). A consequence of the mesh shape is that the variation of h with w is nonlinear when the mesh deforms. Moreover, the h–w relationship depends on the orientation of the deformation. For instance, a 10% increase in the mesh height corresponds to a 20% mesh reduction in width, whereas a 10% increase in the mesh width corresponds to only a 9% reduction in mesh height. Two wire mesh orientations will therefore be considered in order to investigate the influence of this feature on the cell response.

The fill material was contained in the cage by a needle-punched geotextile, 600 g/m^2 in mass per unit area. This geotextile has a tensile modulus of 35 kN/m and a rupture strain of approximately 85%. Two installation procedures were considered for the lateral

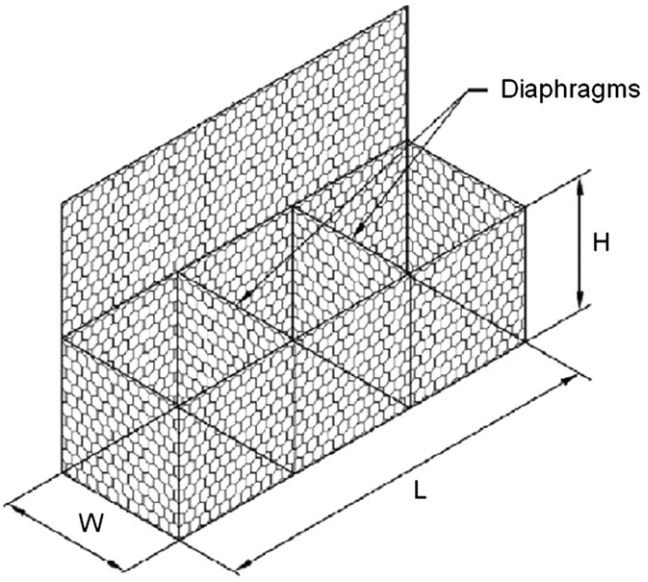

Fig. 1. Gabion cage made of a hexagonal wire mesh.

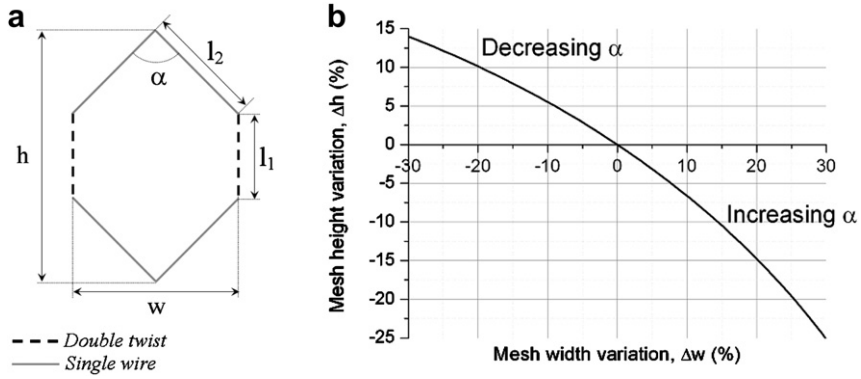

Fig. 2. The mesh: (a) Definitions of w, h, α, l_1 and l_2, (b) l_1 and l_2 remaining constant, the mesh can undergo large deformations; $h-w$ curves display nonlinearities.

containment. The first involved placing eight overlapping square pieces of geotextile on the sides with the aim of reducing the geotextile's influence on the cell response. The second method was only used for 300-mm-high cells and involved using a 1.5-m-long strip of geotextile, overlapping the entire length of one lateral side of the cell.

The fill materials were Hostun sand and scrapped tires.

Hostun sand is a French standard fine angular siliceous sand. It is well-graded and has a size distribution ranging from 0.08 to 1 mm, a mean particle size (d_{50}) = 0.35 mm, an effective particle size (d_{10}) = 0.25 mm, a minimum void ratio (e_{min}) = 0.65, a maximum void ratio (e_{max}) = 0.92, a maximum density = 16 kN/m^3, and a minimum density = 13.3 kN/m^3. The peak friction angle of the sand at 80% relative density was obtained from triaxial compression tests as equal to 35°.

Scrapped tires are obtained by puncturing end-of-life car and truck tires. This material contains 30% by mass circular pieces measuring 25 mm in diameter and are a mean 10 mm thick, and the rest had no particular shape. Its unit weight is approximately 5.5 kN/m^3. Additional data is provided in Gotteland et al. (2005, 2007). This material was chosen both for waste recycling purposes and to take advantage of its particular characteristics, very different from the properties of more classical granular geomaterials.

These fill materials were employed separately and as mixtures containing 30% and 50% by mass of tire.

2.2. Cell preparation

The wire netting panels were connected using standard staples to form the cubic cages, approximately 500 mm and 300 mm on a side. The actual initial height of the cells, H_0, depends on the size of the mesh (Table 2).

The cages were mounted without the internal connecting wires that are generally placed across gabions to reduce the deformation of the lateral sides. The cages were then placed in a wooden box in order to restrict any lateral deformation during filling.

Table 1
Characteristics of the wire nettings used for the different cells.

Wire diameter (mm)	Mesh size $w \times h$ (mm × mm)	Tensile resistance		Cell height (mm)
		Parallel to twist (kN/m)	Perpendicular to twist (kN/m)	
2.7	80 × 100	58	19	500
2.2	60 × 80	36	16	300

The geotextile was then put in place before pouring the dry fill material in three layers. Care was taken to obtain a uniform tire distribution in the cell. For specimens containing 0 and 30% by mass of tire, each layer was gently compacted using a hand-operated hammer. Mixtures containing 50% by mass of tire were not compacted because this process led to heterogeneous specimens as a result of the downward sand migration in this high-void-ratio material. Compaction had no effect on specimens made of tire only. Specimens containing 0, 30%, 50% and 100% by mass of tire had a unit weight of approximately 16, 13.5, 9 and 5.5 kN/m^3, respectively. This parameter is not precisely known since the volume actually occupied by the fill material could not be measured accurately.

2.3. Testing procedure

The investigation of the static response of the cells was based on uniaxial compression tests performed at a constant strain rate of 1%/min (Fig. 3). The force applied on the cell and the loading plate displacement was measured continuously during compression.

As for the intended use, the cells are expected to undergo large deformations. The test on 500-mm-high cells was conducted until a 300-mm load-plate displacement was reached. The axial strain was calculated as the ratio between the load-plate displacement and the current cell height, H. The axial stress was calculated as the ratio between the axial force and the current cell cross-sectional area.

The lateral displacement, d, at the mid-height of the cell was measured continuously on two different sides (Fig. 3(a) and (b)). In the following, only the average value is presented. In order to complement this information, the lateral deformation of the wire netting panels on the sides of the cell was also recorded. A flexible ruler was used to measure the lengths of (i) the vertical median line, (ii) the horizontal median line, which is one-quarter the cell

Table 2
Test cases.

Case	Fill material Tire/sand mass ratio	Initial cell height, H_0 (mm)	Cell mass (kg)
A	0/100	530	217
B	30/70	530	180
C	50/50	530	110
D	100/0	530	66
E[a]	30/70	530	180
F	0/100	290	50
G[a]	0/100	290	50

[a] See the text for comments.

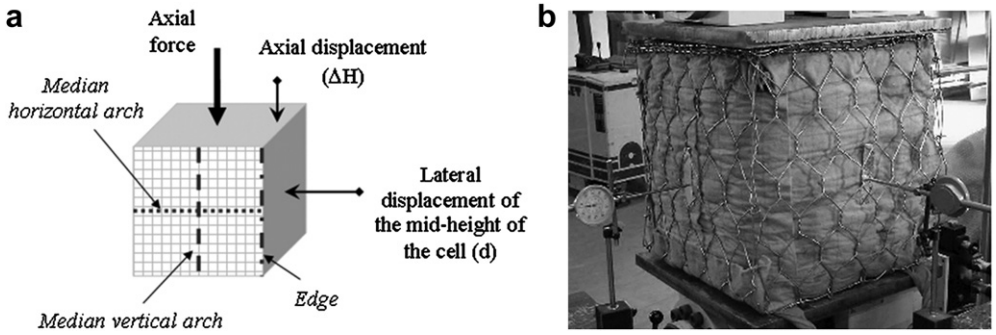

Fig. 3. Compression test: (a) test principle and measurements, and (b) cell at the beginning of the test.

perimeter, and (iii) the vertical edges between two lateral sides (Fig. 3(a)).

The volume change of the cell was estimated based on the above-mentioned measurements using a geometrical description model. This model is based on the assumption that both the median horizontal arch and the median vertical arch describe a portion of a circle and that the four lateral panels deform in the same way. The radii of these circles are calculated from the cell height and lateral displacement measurements. The geometry of the deformed cell is thus accurately obtained, so that its volume can be calculated up to an axial strain of 70%. This model also provides the cell's vertical edge length and the length of both the vertical and horizontal median arches. This makes it possible to compute the cell's cross-section for calculating the axial stress. This model will be validated by comparing the geometrical measurements with the predictions from the model.

2.4. Testing program

A total of 15 tests were performed in different test conditions (Table 2).

Test cases A–D differed in the cell fill material. Case E tested cells similar to case B cells but with the wire netting of the lateral sides turned 90°. In case E, the height of the hexagon of the mesh was aligned with the horizontal axis (horizontal orientation).

The tests of cases G and F were performed on 300-mm-high cells to investigate the influence of the continuity of the lateral containment geotextile on the cell response: the containment is discontinuous for case F cells and continuous for case G cells. This cell dimension is not representative of real site conditions.

Cases A–F included two tests. The two curves were checked for similarity and only one is presented in the following. Three tests were performed for case G for repeatability reasons.

3. Test results and analysis

Fig 4 shows the stress vs. strain curves during the compression of cells filled with the different materials (cases A–D) either focusing on low and high axial strains.

For strain states of less than 25% (Fig. 4a), the cell response was significantly affected by the fill material. In particular, the cell filled with the 30% tire mixture exhibited higher axial stress values. The cells filled with sand and with the 30% tire mixture showed a pronounced peak at an axial strain of 9 and 11%, respectively.

Above a 25% axial strain, the stress increased nearly exponentially for all the fill materials (Fig. 4b). The increase rate depended on the tire content: the higher the tire content, the lower the increase rate. The tire content also strongly affected the lateral displacement of the cell (Fig. 5).

Fig. 6 illustrates the changes in the shape of a cell filled with sand during the compression test as deduced from the measurements on the cell sides. The median vertical arch length decreased, as did the edge length, whereas the length of the median horizontal arch increased. This means that the perimeter of the cell increased, reaching more than 140% of the initial length. In fact, meshes along

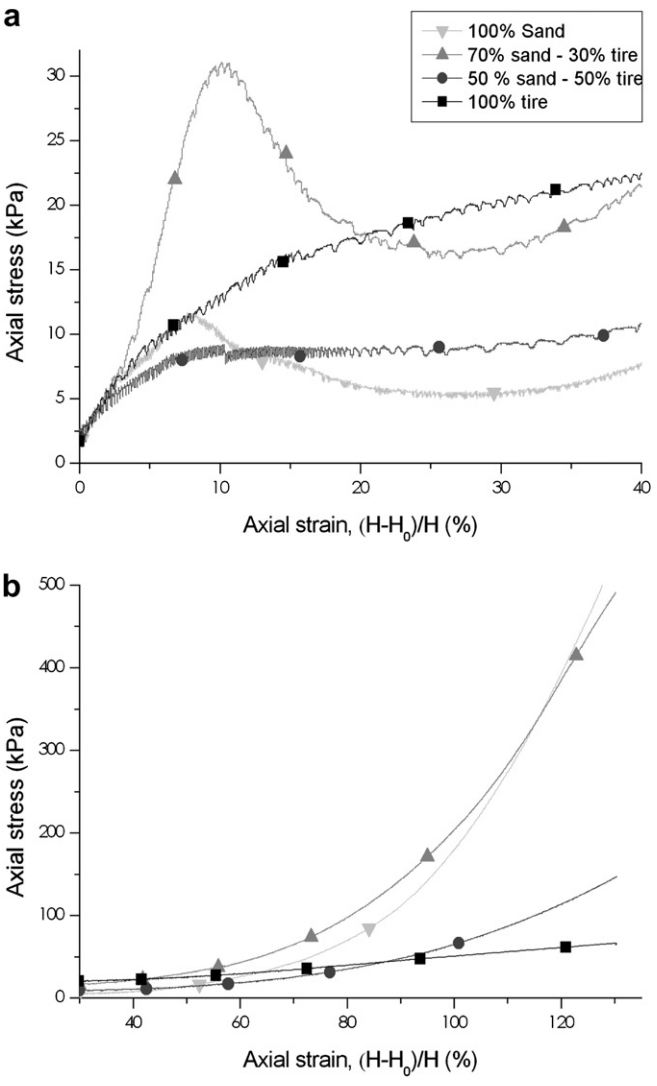

Fig. 4. Stress vs. axial strain curves for 500-mm-high cubic cells filled with different tire–sand mixtures, cases A–D: (a) at low axial strain and (b) high axial strain.

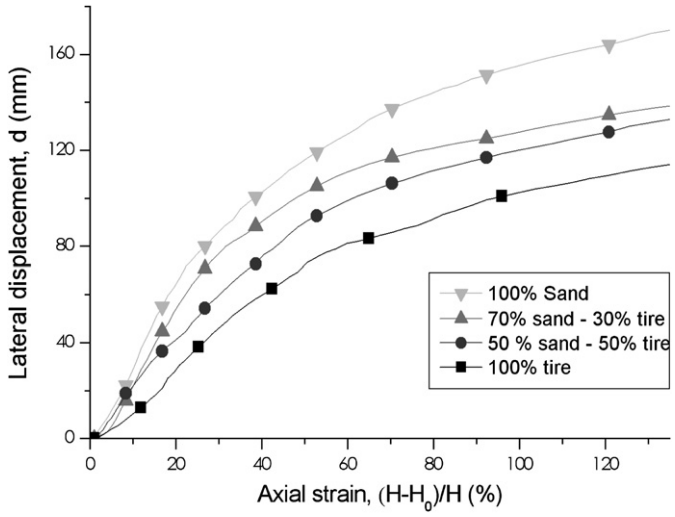

Fig. 5. Displacement of the center of the lateral sides of the cell for 500-mm-high cubic cells filled with different tire–sand mixtures, cases A–D.

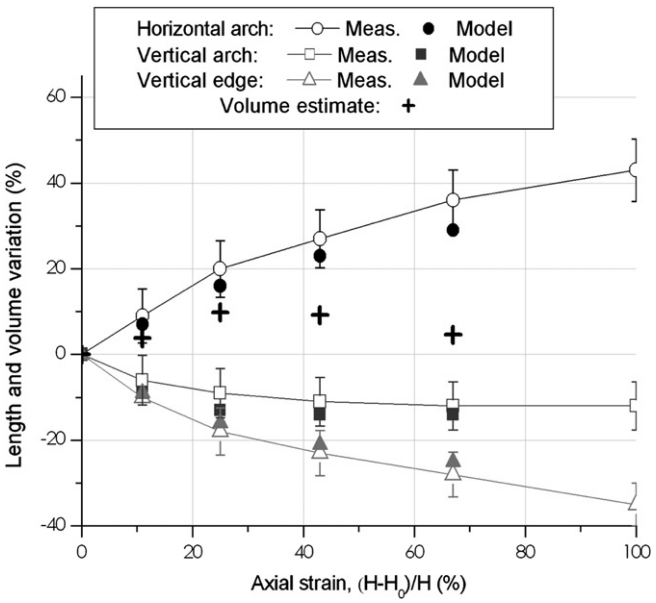

Fig. 7. Geometrical measurements compared to the model predictions (case A).

this perimeter underwent substantial deformations at high cell axial strain. The greatest mesh deformations were an approximately 50% width increase and a 20% height decrease in the cells filled with sand (case A).

These length changes were well predicted by the volume estimation model (Fig. 7) for cells filled with sand (case A). This confirms the relevance of the model and allows for considering the volume estimation. When subjected to uniaxial compression, Fig. 6 shows that a cubic cell first undergoes a volume increase, with an apex reached for a 30% axial strain before decreasing.

For the other fill materials, the agreement between geometrical measurements and predictions is not good enough to estimate the cell volume. In fact, the model cannot capture the actual cell deformation satisfactorily because the assumptions on the shape of the cell are not appropriate. This shows that the lateral displacement of the cell walls is not sufficient for estimating the cell shape for any fill material. In addition, for a given axial strain the dimensions of the cell's lateral sides depend to a large extent on the fill material.

Finally, the important feature in the stress-strain curves is that the stress increases exponentially from a 25% axial strain, which corresponds to the cell volume apex.

Fig. 8 illustrates the influence of wire mesh orientation on the cell response. Case B tests were compared to case E tests, with the latter corresponding to cells for which the wire mesh was turned 90°. Turning the lateral wire netting panels substantially changes the response of the cell, increasing the axial stress beginning with an axial strain of 10%. The curve concerning the cell made of turned wire netting panels exhibits small amplitude stress variations from 50% axial strain. These are caused by the progressive opening of the staples as a result of excessive loading.

The difference in wire netting orientation also affects the cell's shape, as presented in Fig. 9, giving the median vertical arch length variation vs. the median horizontal arch length variation.

Both curves reveal an increase in the length of the horizontal arch and a reduction in the length of the vertical arch. With a wire mesh oriented horizontally, a 12–13% vertical arch shortening corresponds to a lengthening of the horizontal arch by 10%. In contrast, the same vertical arch shortening corresponds to lengthening the horizontal arch by 20% with the wire mesh oriented vertically.

This means that in the first case, the perimeter lengthening, and thus the lateral expansion is reduced, suggesting a higher confinement effect with the wire mesh turned 90° (horizontal mesh orientation).

Fig. 9 also presents the deformation of a single hexagonal mesh resulting from the wire-bending mechanism described above (Section 2.1), with either an increase in mesh height, *h*, or an increase in mesh width, *w*, as depicted in Fig. 2(b). This figure shows that at the beginning of cell compression, the deformation of the horizontally oriented mesh panel follows the deformation of a single mesh elongated along its height (square symbols). Inversely, the deformation of the vertically oriented mesh panel follows the deformation of a single mesh elongated along its width (circles). This result tends to prove, as far as the beginning of the compression loading is concerned, that the netting panel's

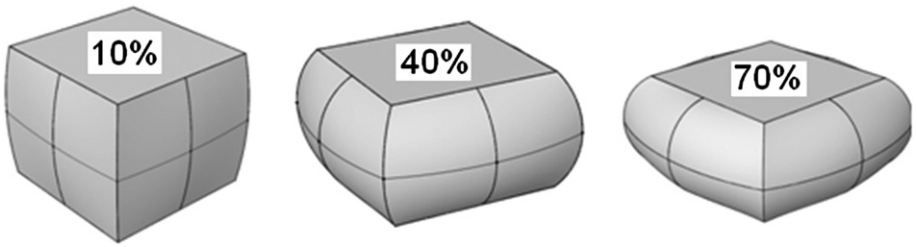

Fig. 6. Illustration of the deformation of a geocell filled with sand (case A) subjected to a uniaxial compression test for a 10, 40 and 70% axial strain.

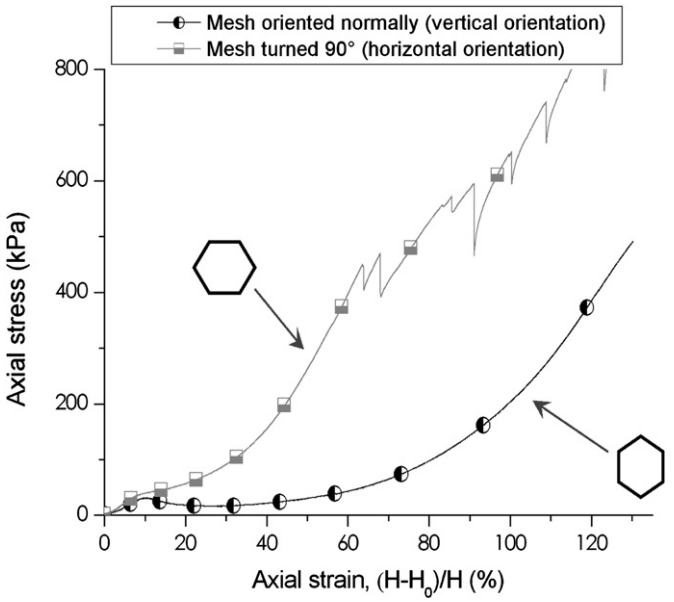

Fig. 8. Influence of the orientation of the lateral side wire netting mesh panels on the geocell response (cases B and E).

deformation mainly results from the wire-bending mechanism. For higher strain levels, the volume increase of the fill material induces tensile mechanisms within the envelope, causing the discrepancies observed in Fig. 9 beyond 20% length variation.

The evaluation of the influence of the discontinuity of the containment geotextile is based on test cases F and G, both using 300-mm-high cells filled with sand (Fig. 10). Despite great variability in responses from one cell to another, the influence of wrapping continuity is clearly shown. The axial stress started increasing for a lower strain with a continuous strip of geotextile. It is worth noting that for case G cells, substantial sliding was observed in the overlapping area. At the end of the test, sliding accounted for as much as one-third of the perimeter lengthening. This sliding resulted from excessive tensile stress in the envelope and consequently reduced the confining effect.

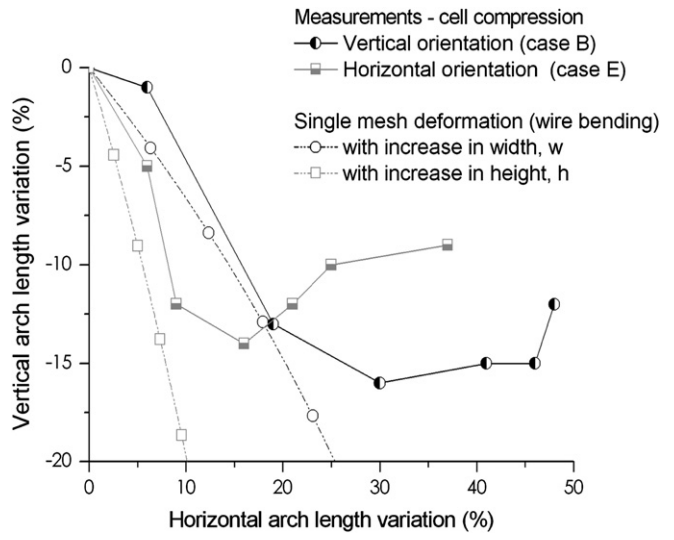

Fig. 9. Deformation of the lateral sides of the cells of cases B and E compared to the deformation of a single hexagonal mesh resulting from bending at the wire connections (open symbols).

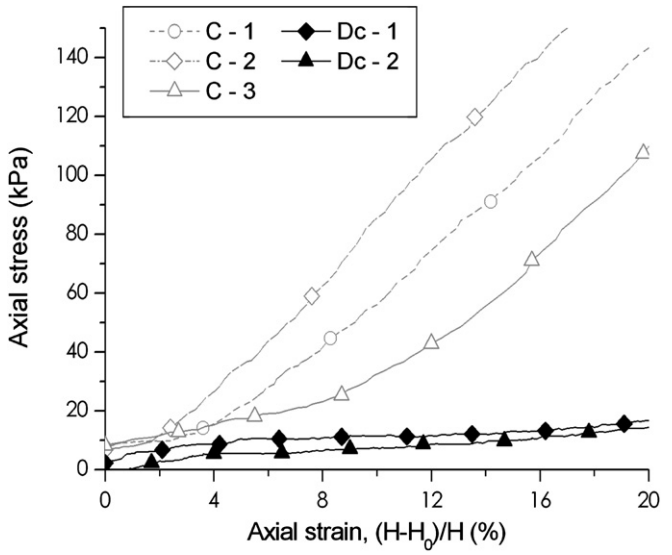

Fig. 10. Influence of the continuity of the lateral containment geotextile. Filled symbols stand for discontinuous (Dc) pieces of geotextile (case F), open symbols stand for a continuous (C) strip of geotextile (case G).

These results suggest that the discontinuous geotextile makes no contribution to the cell's bearing capacity.

4. Discussion

4.1. Low axial strain cell response

The cell's response to low axial strain is mainly governed by the mechanical characteristics of the fill material. Indeed, stress vs. strain curves with up to 15% axial strain exhibit similar trends as observed in previous studies based on triaxial tests performed on tire–sand mixtures (Zornberg et al., 2004). Gotteland et al. (2005) reported that the optimum in terms of shear resistance was obtained for a 30% by mass tire–sand mixture and that the peak deviator was reached at a higher strain with this mixture than with sand alone.

The stress vs. strain curves suggest that the effect from the envelope remains relatively constant at the beginning of compression. The confining stress resulting from this effect can be estimated by considering the specimen to be a cylinder and with the fill material subjected to a triaxial loading path.

With sand (case A), the peak observed at 9% axial strain can be considered to correspond to the plastic limit. At the peak, both axial and lateral stresses, σ_1 and σ_3, respectively, are therefore related by:

$$\sigma_1 = \sigma_3 \tan^2\left(\frac{\pi}{4}+\frac{\phi}{2}\right) \quad (3)$$

where ϕ is the friction angle of the sand.

For sand, Fig. 4 indicates that at a 9% cell axial strain σ_1 equals 12 kPa. The friction angle of the sand being 35°, Eq. (3) gives a value of about 3 kPa for the confinement stress due to the envelope, σ_3. This value appears to be very low compared to previously published values (Rajagopal et al., 1999; Madhavi Latha et al., 2006), confirming that the envelope effect remains small at low axial strains. As a consequence, the load-carrying capacity of the cells is low.

4.2. High axial strain cell response

The progressive cell height reduction leads to its lateral expansion, inducing a strain in the envelope. This effect results in

a confining stress on the fill material, and thus to an increase in the axial stress.

When the mesh is oriented vertically, the axial stress increases exponentially from a strain of about 25%, whereas it increases from an axial strain of about 10% when the mesh is oriented horizontally. This difference stems from the hexagonal shape of the mesh. This type of mesh can reach high levels of strain simply by bending at the wire connections, with a significant dependence on the mesh orientation (Fig. 2). As a result of this feature, a mesh oriented vertically on the cell side is prone to a higher deformation along the cell perimeter than a mesh oriented horizontally. This gives rise to a greater cell volume increase at the beginning of compression and then to a longer delay of the confinement effect.

Actually, the lateral envelope experiences necking with lengthening along the perimeter and shortening along the perpendicular direction. This contrasts with certain standardized uniaxial tensile tests on industrial products where necking is restricted. The consequence is that in the case of an envelope material prone to necking, such as wire mesh or certain geotextiles, the results from such tests are not appropriate when quantifying the confining effect using Eq. (1), for instance.

The second reason for this delay is that the geotextile is discontinuous. In this case, its contribution to the confinement effect is minor because overlapping pieces of geotextiles slide and the tension forces developed within are small. In contrast, a continuous strip of geotextile contributes to the confinement, eliminating this confinement effect delay.

The last reason for this delay, although not investigated, is the shape of the cell. Axial stress vs. strain curves on case E cells still exhibit an approximately 10% delay in axial strain. It is assumed that this is caused by the cell's cross-sectional shape. It must deform before efficiently inducing a hoop tension effect in the envelope, which is not true if the initial cross-section is circular (Bathurst and Rajagopal, 1993; Pokharel et al., 2010). This explains that in the absence of the internal connecting wires that are usually placed across gabion cells, the load-carrying capacity measured at low strains is relatively low.

4.3. Volumetric behavior

Beyond the axial strain required to efficiently mobilize the envelope effect, the cell response reveals the competition between the volumetric behavior of the fill material and the volumetric behavior of the envelope.

At high strain, the envelope deforms so that its volume reduces. The fill material may counter this trend, leading to an increase in the cell's load-carrying capacity.

Nevertheless, this counter-effect is reduced with materials containing more than 30% by mass of tire (Gotteland et al., 2005). As these materials are prone to contraction, the lateral expansion of the cell is smaller and the resulting force acting on the envelope is reduced. This emphasizes the importance of the dilatancy of the fill material, as discussed in previously published studies showing the influence of fill material compaction on the cellular structure response (Iizuka et al., 2004; Dash, 2010). This parameter may be accounted for as proposed by Iizuka et al. (2004). Moreover, Eq. (1) provided by Henkel and Gilbert (1952) may not be fully satisfactory because it is based on the assumption that the fill material volume remains constant.

4.4. Practical implications

The cells studied are intended to be part of innovative sandwich rockfall protection structures with, most particularly, the granular fill material depending on the cell location (Nicot et al., 2007; Lambert et al., 2009). The aim is to improve the structure's ability to dissipate energy and dampen the impact force. This implies that the cell deforms during the impact and that the cell's reaction force does not greatly increase during the impact.

In this context, the envelope should ensure the containment of the fill material while not affecting the mechanical characteristics of the cell during the impact by the rock boulder.

The results presented in this paper show that for any fill material, the envelope confining effect does not affect significantly the load-carrying capacity of the cell up to a 25% axial strain. This beneficial consequence of the mesh shape is obtained providing the lateral wire mesh panels are normally oriented and that the lateral containment geotextile is discontinuous. This confirms the conclusions drawn by the authors based on cell impact experiments (Lambert et al., 2009). Below a certain deformation limit, the cell's reaction to the impact by the boulder was not affected by the envelope but was governed by the fill material's characteristics. This type of envelope may therefore be appropriate for building sandwich rockfall protection structures.

5. Conclusion

The purpose of this study was to assess the interaction between a cubic envelope made up of a hexagonal wire mesh combined with a containment geotextile and different fine granular noncohesive fill materials. The fill materials were sand and scrapped tires used alone or as mixtures. This investigation has brought out important features that should be accounted for in view of developing a constitutive model for these cells. Based on experimental tests, phenomenological results have been obtained that are believed to take place in the dissipation mechanism within cells during impacts. The next step would be incorporating these new phenomenological ingredients into a constitutive model.

The single-cell response under uniaxial compression appears to strongly depend on the fill material's characteristics for low axial strains. The axial stress increases exponentially after 25% axial strain as a result of the confining effect of the envelope. The confinement effect is delayed due to the shape of the mesh. For this reason, this type of material containment is suitable for the construction of protection structures where large deformations are expected and where the aim is to reduce the impact force.

More generally, the conclusions drawn from these experiments concerning the cell envelope-fill material interaction are as follows.

- The confining effect results from the competition between the evolution of the volume inside the envelope and the volumetric behavior of the fill material.
- The volumetric behavior of the fill material should be considered when designing cellular structures: the confining effect is significantly reduced when a contractant fill material is used.
- Possible necking of the envelope material should be considered when assessing the confining effect, as necking may delay the confining effect.
- The previous points highlight the importance of extending the currently used envelope-fill material interaction model (Henkel and Gilbert, 1952), accounting for the change in volume inside the envelope.

Acknowledgements

This research was completed within the REMPARe project, funded by the French National Research Agency (ANR). The authors would like to thank the Technological University Institute of Grenoble (A. Petronne) for technical assistance.

References

Bathurst, R.J., Rajagopal, K., 1993. Large-scale triaxial compression testing of geocell-reinforced granular soils. Geotechnical Testing Journal 16, 296–303.

Bergado, D.T., Voottipruex, P., Srikongsri, A., Teerawattanasuk, C., 2001. Analytical model of interaction between hexagonal wire mesh and silty sand backfill. Canadian Geotechnical Journal 38, 782–795.

Bourrier, F., Gotteland, P., Nicot, F., Lambert, S., 2010. A model for rockfall protection structures based on a multi-scale approach. In: Proceedings of Geoflorida 2010, West Palm Beach, Florida, USA, pp. 2281–2290.

Chen, R.H., Chiu, Y.M., 2008. Model tests of geocell retaining structures. Geotextiles and Geomembranes 26, 56–70.

Dash, S.K., 2010. Influence of relative density of soil on performance of geocell-reinforced sand foundations. Journal of Materials in Civil Engineering 22 (5), 533–538.

Gotteland, P., Lambert, S., Balachowski, L., 2005. Strength characteristics of tyre chips-sand mixtures. Studia Geotechnica et Mechanica 27, 55–66.

Gotteland, P., Lambert, S., Salot, C., Gras, V., 2007. Investigating the strength characteristics of tyre chips sand mixtures for geo-cellular structure engineering. In: Proceedings of International Workshop on Scrap Tire Derived Geomaterials – Opportunities and Challenges, Yokosuka, Japan, pp. 351–361.

Henkel, D.J., Gilbert, G.D., 1952. The effect of the rubber membrane on the measured triaxial compression strength of clay samples. Geotechnique 3, 20–29.

Iizuka, A., Kawai, K., Kim, E.R., Hirata, M., 2004. Modeling of the confining effect due to the geosynthetic wrapping of compacted soil specimens. Geotextiles and Geomembranes 22, 329–358.

Lambert, S., Gotteland, P., Nicot, F., 2009. Experimental study of the impact response of geocells as components of rockfall protection embankments. Natural Hazards and Earth System Sciences 9, 459–467.

Madhavi Latha, G., Rajagopal, K., Krishnaswamy, N.R., 2006. Experimental and theoretical investigations on geocell-supported embankments. International Journal of Geomechanics 6, 30–35.

Muhunthan, B., Shu, S., Sasiharan, N., Hattamleh, O.A., Badger, T.C., Lowell, S.M., Duffy, J.D., 2005. Analysis and Design of Wire Mesh/Cable Net Slope Protection. Technical Report WA-RD 612.1. Washington State Transportation Commission.

Nicot, F., Gotteland, P., Bertrand, D., Lambert, S., 2007. Multi-scale approach to geocomposite cellular structures subjected to impact. International Journal for Numerical and Analytical Methods in Geomechanics 31, 1477–1515.

Peyras, L., Royet, P., Degoutte, G., 1992. Flow and energy dissipation over stepped gabion weirs. Journal of Hydraulic Engineering 118, 707–717.

Pokharel, S.K., Han, J., Leshchinsky, D., Parsons, R.L., Halahmi, I., 2010. Investigation of factors influencing behavior of single geocell-reinforced bases under static loading. Geotextiles and Geomembranes 28, 570–578.

Rajagopal, K., Krishnaswamy, N.R., Madhavi Latha, G., 1999. Behaviour of sand confined with single and multiple geocells. Geotextiles and Geomembranes 17, 171–184.

Scherbatiuk, K., Rattanawangcharoen, N., Pope, D.J., Fowler, J., 2008. Generation of a pressure-impulse for a temporary soil wall using an analytical rigid-body rotation model. International Journal of Impact Engineering 35, 530–539.

Turk, G.F., 2001. Testing and Evaluation of a New Expedient Structure for Flood Fighting-Rapidly Deployed Fortification Wall (RDFW). Technical Report ERDC-GL-00–01. US Army Corps of Engineers.

Webster, S.L., 1979. Investigation of Beach Sand Trafficability Enhancement Using Sand-grid Confinement and Membrane Reinforcement Concepts. Technical Report GL-79–20. US Army Corps of Engineers, Vicksburg, MS.

Wesseloo, J., Visser, A.T., Rust, E., 2009. The stress–strain behaviour of multiple cell geocell pack. Geotextiles and Geomembranes 27, 31–38.

Yuu, J., Han, J., Rosen, A., Parsons, R.L., Leshchinsky, D., 2008. Technical review of geo-cell-reinforced base courses over weak subgrade. In: Proceedings of the First Pan American geosynthetics conference, Cancun, Mexico, pp. 1022–1030.

Zhang, L., Zhao, M., Shi, C., Zhao, H., 2010. Bearing capacity of geocell reinforcement in embankment engineering. Geotextiles and Geomembranes 28, 475–482.

Zornberg, J., Cabral, A., Viratjandra, C., 2004. Behaviour of tire shred-sand mixtures. Canadian Geotechnical Journal 41, 227–241.